Journal of The Electrochemical Society, **147** (11) 4229-4238 (2000)
S0013-4651(00)05-094-1 CCC: $7.00

Catalytic Effect of Platinum on Oxygen Reduction
An *Ab Initio* Model Including Electrode Potential Dependence

Alfred B. Anderson*,z and Titus V. Albu

Department of Chemistry, Case Western Reserve University, Cleveland, Ohio 44106-7078, USA

The effects of bonding to a platinum atom are calculated for the reduction of oxygen to water. The electron-correlation corrected MP2 method is used, and the electrode potential is modeled by variations in values for the electron affinities of the reaction centers. Potential–dependent transition state structures and activation energies are reported for the one-electron reactions

$$Pt–O_2 + H^+(aq) + e^-(U) \rightarrow Pt–OOH \quad [i]$$

$$Pt–OOH + H^+(aq) + e^-(U) \rightarrow Pt–(OHOH) \quad [ii]$$

$$Pt–(OHOH) + H^+(aq) + e^-(U) \rightarrow Pt–OH + H_2O \quad [iii]$$

$$Pt–OH + H^+(aq) + e^-(U) \rightarrow Pt–OH_2 \quad [iv]$$

This is the predicted lowest energy pathway. An alternative, where step (*ii*) is replaced by

$$Pt–OOH + H^+(aq) + e^-(U) \rightarrow Pt–O + H_2O \quad [v]$$

is excluded by the high activation energy calculated for it, though reduction of Pt–O to Pt–OH

$$Pt–O + H^+(aq) + e^-(U) \rightarrow Pt–OH \quad [vi]$$

has a very low activation energy. Compared to uncatalyzed outer-Helmholtz–plane values, bonding to the Pt has the effect of decreasing the calculated high reduction activation energies for O_2 and H_2O_2. Bonding to Pt also decreases the HOO· and increases the HO· activation energy values. The reverse reaction, oxidation of H_2O to O_2, is also discussed in light of these results. The issues of potential–dependent double–layer potential drops and adsorbate bond polarizations are discussed, and it is pointed out that the results of this study can be used to estimate the effects of such potential drops.

Manuscript submitted May 30, 2000; revised manuscript received July 27, 2000.

Platinum has long been the best electrocatalyst for oxygen reduction, and oxygen reduction over platinum[1,2] and other[2] surfaces has been reviewed recently by Markovic and Ross[1] and Adzic.[2] As discussed in these reviews, over the three low-index (100), (111), and (110) platinum surfaces in aqueous perchloric and sulfuric acid, the complete four-electron reduction to water can be observed. In the hydrogen adsorption region, two-electron reduction to hydrogen peroxide occurs on the (111) surface, evidently a result of surface site blocking by H(ads). OH(ads), which begins forming from water decomposition at about 0.6 V on platinum electrodes, is also believed to inhibit oxygen reduction by blocking surface sites, and it may contribute to the need to operate oxygen electrodes at several hundred millivolts overpotential relative to the 1.23 V reversible potential on the standard hydrogen scale, which is the scale used in this paper. Surface blocking by adsorbed foreign atoms sometimes changes the reduction of oxygen from the four-electron production of H_2O to the two-electron production of H_2O_2, and when this occurs it is thought to be due to changing the initial O_2 adsorption from side-on to end-on.[3-5] Recent work has pointed to bisulfate and other ions as surface blocking agents and has found, based on the temperature dependence of exchange currents extrapolated from Tafel plots in the double-layer region, an activation enthalpy of 0.44 eV for O_2 reduction at the reversible potential in 0.05 M sulfuric acid for the three low-index Pt surfaces.[1,6] These findings were said to indicate that a "series" mechanistic pathway is followed over the Pt surfaces with the first electron transfer being rate determining and OOH(ads) being an intermediate.[1,6]

Additional experimental or theoretical information on the mechanism, particularly to elucidate the relationship between electron and proton transfer, is needed to establish the mechanism. Though a small number of semiempirical quantum chemical studies have been made of some of the steps,[7-10] there has been little accurate theoretical work on oxygen reduction over platinum and other metal surfaces. Contributing to the paucity of activity has been the lack of an *ab initio* charge self-consistent theory for electrocatalysis that includes the dependence of mechanisms, structures, and activation energies on the potential of the electrode. This laboratory has recently been developing such an approach to studying the electrode potential dependence of electrochemical reactions. Previous applications were on hydrogen evolution from conducting diamond film cathodes,[11] and on oxygen reduction in the outer-Helmholtz–plane region.[12,13] In this paper the catalytic effects of platinum on oxygen reduction are considered.

There are two widely used phenomenological models for relating electrode currents to activation Gibbs energies. Both take the point of view of expanding the activation Gibbs energy about the reversible potential. The linear approximation gives rise to the Butler-Volmer equations[14] and provides insight into the linear regions of Tafel plots of the log of the current density *vs.* the applied electrode overpotential. The harmonic model has linear and quadratic terms and a parameter attributed to the solvent reorganization energy that accompanies the electron transfer process.[15,16] This model has been incorporated into quantum-mechanical-based electron-transfer equations by Marcus, Gerischer, Levich and Dogonadze, and others[15,16] for characterizing outer–sphere electron–transfer reactions where electron tunneling is associated with a sudden charge in redox state, a model originally suggested by Gurney.[17] Hush introduced an adiabatic electron-transfer model for redox centers in contact with the electrode surface and showed how it can relate to the harmonic model.[18] Adiabatic models have been employed by Schmickler and others to treat surface-activated inner-Helmholtz plane redox reactions,[19] and Koper and Voth have obtained approximate activation energies at different potentials for the electrode–surface mediated reduction of Cl_2.[20] The pre-exponential term in the electron-transfer rate constant is generally treated through the use of the two-state

* Electrochemical Society Active Member.
z E-mail: aba@po.cwru.edu

S0013-4651(00)05-094-1 CCC: $7.00

model involving an electron donor wave function and acceptor wave function and their coupling through the electron transfer integral. Newton has reviewed the coupling formalism.[21]

The present paper and its predecessors[11-13] provide a theoretical approach to the potential dependence of redox activation energies alone, pre-exponential factors not being treated in this work. The current model simply assumes, as is discussed below, the formation of an electronic equilibrium between the transition state complex and the electrode at each potential U.

In the outer-sphere oxygen reduction study[12,13] the following four steps were modeled

$$O_2(g) + H^+(aq) + e^-(U) \rightarrow HO_2\cdot(aq) \quad [1]$$

$$HO_2\cdot(aq) + H^+(aq) + e^-(U) \rightarrow H_2O_2(aq) \quad [2]$$

$$H_2O_2(aq) + H^+(aq) + e^-(U) \rightarrow HO\cdot(aq) + H_2O(aq) \quad [3]$$

$$HO\cdot(aq) + H^+(aq) + e^-(U) \rightarrow H_2O(aq) \quad [4]$$

Predicted activation energies for outer-sphere O_2 reduction decreased as the electrode potential decreased for all four steps. H_2O_2 reduction, Eq. 3, had the highest activation energy, with O_2 reduction activation energy, Eq. 1, about 0.5 eV smaller and those for HOO· and HO· reduction, Eq. 2 and Eq. 4, respectively, being still smaller. These results seemed consistent with the observed ability of weakly interacting electrodes like hydrogenated platinum[2] or mercury[22] to release hydrogen peroxide.

It should be noted that the activation enthalpies and activation energies for reactions treated in this paper are practically identical. Experimentally determined activation enthalpies in Ref. 6 were obtained from Arrhenius–type plots. The $p\Delta V$ terms that must be subtracted from these activation enthalpies to yield activation energies are small for these reduction reactions, around 1 J, based on an activation volume change of $\sim$10 mL mol^{-1}.[23]

An electrocatalyst surface should, at least, lower the activation energy for hydrogen peroxide reduction and may also activate the first step of oxygen reduction. The purpose of the present study is to gain understanding of the electrocatalytic ability of platinum and, in this initial exploratory study, the above four steps and two additional ones are examined with all intermediates bonded to a platinum atom. Two new issues must be addressed in considering the application of this theory for oxidation and reduction of species that are bonded to the electrode surface: (*i*) the possible potential drops across the double layer and how they may vary with the applied potential and (*ii*) the potential dependent polarization of adsorbate bonds. These are also discussed in this paper.

Theory

Electron transfer and electrode potential.—The electron is assumed to come from an electron donor D, with electron chemical potential μ(D). The reduction center, R, an example for this being $[OO\cdots H\cdots OH_2(OH_2)_2]^+$ in the first step of O_2 reduction to water, has an electron affinity, E_a(R), which depends on its structure. Due to thermal fluctuations, R will pass through structures for which its electron affinity matches the electron chemical potential of the donor. For these structures, it is assumed that electron transfer takes place by radiationless tunneling

$$D + R' \rightarrow D^+ + R'^- \quad [5]$$

where R′ stands for the reactant in this activated structure. Following electron transfer the reaction can continue to form the reduction product.

The electron chemical potential of the electrode is the negative of the thermodynamic work function, φ

$$\mu = -\varphi \quad [6]$$

On the standard hydrogen electrochemical scale this will correspond to an electrode potential $U(V)$ given as

$$U/V = \varphi/eV - \varphi_{H^+/H_2}/eV \quad [7]$$

where φ_{H^+/H_2} is the thermodynamic work function of the standard hydrogen electrode. Using the average value[24] of 4.6 eV for φ_{H^+/H_2} and $-\mu$(D) for φ

$$U/V = -\mu(D)/eV - 4.6 \quad [8]$$

The energy of R is dependent on structure, as is its electron affinity, which is determined by the energy difference between energy of R and energy of R^- with the same structure. The calculations in this study proceed by identifying structures where $E_a(R') = \sim\mu(D)$ and searching for the lowest energy one.[12,13] This procedure specifies the electron-transfer state for the corresponding potential given by Eq 8. For the studied systems, this structure also corresponds to the transition state, because of the bond order changes that accompany the electron transfer. The transition state and its energy minus the reactant energy gives the activation energy that is predicted by this approach. Since such transition states are at the intersection of two energy surfaces, they are not characterized by saddle points with negative second derivatives as is the case for transition states over a fixed electronic state energy surface. Note that because the donor is isolated from the reduction center, it need not be explicitly present in the energy computation, as it was in Ref. 11, to carry out this procedure and no explicit donor is used in the present work.

Computational model.—The MP2 method,[25] employed in the frozen core approximation in the earlier study of outer-sphere oxygen reduction and water oxidation,[12,13] is used for this work with a 6-31G** basis set for O and H atoms and LANL2DZ for the Pt atom. A single platinum atom is used for coordinating O_2, H_2O, and the HOO·, H_2O_2, and HO· intermediates in the oxygen reduction and water oxidation reactions. While this model does not allow making an analysis of adsorbate properties in the bridge-bonded structures on Pt(111) proposed in the literature,[1-5] it is not as bad a model for the platinum surface as it might first appear to be. Regarding energies, the calculated Pt–OH bond strength, omitting zero-point energies, as done throughout this study, is 2.98 eV, compared to the 2.5 eV low-coverage experimental value.[26] Similarly, the Pt–OH_2 bond strength is calculated to be 0.57 eV, compared to the 0.42 eV experimental value[27] for the (111) surface at low coverage in vacuum.

Regarding electronic properties of platinum, small clusters have large ionization potentials. The ionization potential of the Pt atom is 9.0 eV,[28] whereas the photoelectric work function of polycrystalline Pt is 5.65 eV.[29] The electron affinity of a Pt atom is 2.128 eV.[30] Interestingly, the average of the Pt atom E_a and ionization potential (IP) is 5.6 eV, which is close to φ for the Pt surface. An isolated Pt atom will not accept an electron from an electrode that is at potentials greater than -2.5 V (2.1–4.6 V) and will not donate an electron to an electrode that is at potentials less than 4.4 V (9.0–4.6 V). This means that it is possible to study redox reactions over the range of -2.5 to 4.4 V with a single–Pt–atom model.

Calculated structures for the studied compounds as free molecules and when bonded to the platinum atom are in Table I. The model for the reactant $H^+(aq)$ is a hydronium ion solvated with two water molecules as in the previous work.[12,13] A similar model was also used by Kuznetsov and Lorenz in studying proton adsorption on copper, but without a potential dependence.[31] In determining the structures for the hydrogen–bonded precursors, $R–O\cdots H^+ - OH_2(OH_2)_2$, and for the transition states, $RO\cdots H^+\cdots OH_2(OH_2)_2$, only three geometric parameters are varied: the R–O, $H^+\cdots O$, and $O\cdots O$ distances. Figure 1 illustrates this for the case of H_2O_2. The other structure parameters are constrained as follows: the $O–H^+–O$ angle is 180° and the other bond distances, angles, and dihedral angles are set at the reduction product values. The $OH_2(OH_2)_2$ structure is kept fixed as in previous work.[12,13] Specifically, the activation energies and transition state structures for each studied potential are found by stepping $H^+\cdots O$ and $O\cdots O$ distances in 0.01 Å increments and for each pair of values R–O is varied until the reaction complex $R–O\cdots H^+\cdots OH_2(OH_2)_2$ has the desired electron affinity. The most stable such structure determines the transition state parameters while its energy determines the activation energy.

S0013-4651(00)05-094-1 CCC: $7.00

Table I. Calculated equilibrium internuclear distances, R_e (Å), angles, θ_e (deg), and dihedrals, ϕ_e (deg), for PtO_2, PtOOH, PtOHOH, PtOH, $PtOH_2$, and PtO. O_a represents the oxygen atom bonded to platinum while O_b is the other oxygen atom (Fig. 1). Structures in the absence of Pt are in parantheses.

Molecule	$R_e(Pt–O_a)$	$R_e(O_a–O_b)$	$\theta_e(PtO_aO_b)$	$R_e(O_a–H)$	θ_e (PtO_aH)	$R_e(O_b–H)$	$\theta_e(O_aO_bH)$	$\phi_e(PtO_aO_bH)$
PtO_2 (T-shaped)	1.999	1.417 (1.247)	69.2					
PtO_2 (bent)	1.813	1.341 (1.247)	119.3					
PtOOH	1.848	1.458 (1.326)	112.8			0.972 (0.975)	98.8 (104.4)	100.7
PtOHOH[a]	2.015	1.501 (1.467)	112.3	0.977 (0.968)	105.5	0.977 (0.968)	97.3 (98.6)	6.7
PtOH	1.865			0.976 (0.972)	105.6			
$PtOH_2$[b]	2.058			0.971 (0.961)	103.7			
PtO (triplet)	1.676							
PtO[c] (singlet)	1.724							

[a] HO_aO_bH dihedral is 117.3 (120.4) deg.
[b] HOH angle is 105.9 (103.7) deg.
[c] Experimental singlet value is 1.7273 Å [K. P. Huber and G. Herzberg, *Molecular Spectra and Molecular Structure IV. Constants of Diatomic Molecules*, p. 548, Van Nostrand Reinhold, New York (1979)].

Results and Discussion

Oxygen reduction.—Calculated activation energies for the four reduction steps

$$Pt–O_2 + H^+(aq) + e-(U) \rightarrow Pt–OOH \quad [9]$$

$$Pt–OOH + H^+(aq) + e-(U) \rightarrow Pt–OHOH \quad [10]$$

$$Pt–OHOH + H^+(aq) + e-(U) \rightarrow Pt–OH + H_2O \quad [11]$$

$$Pt–OH + H^+(aq) + e-(U) \rightarrow Pt–OH_2 \quad [12]$$

are graphed with solid connecting lines in Fig. 2 along with the uncatalyzed activation energies for Reactions 1–4, which are connected by dashed lines. It is quickly evident that the Pt atom has a significant effect on the most difficult step of the outer-sphere reaction, reduction of H_2O_2 to HO· + H_2O. Activation energies drop about 1 eV over the 0–2 V potential range studied. Activation energies for the O_2 reduction step are also substantially reduced. The activation energies for HO· reduction to H_2O increase when HO· is bonded to the platinum atom and bonding to Pt decreases the activation energies for HOO· reduction to H_2O_2. In all cases the activation energies are predicted to increase with increasing potential.

The catalytic effects of the platinum atom can be, in part, accounted for by considering the bond strengths between the intermediates and the platinum atom that are given in Table II. O_2 bonds 1.30 eV more weakly to the Pt atom in the end-on orientation than HOO·, and this lowers the activation energy for O_2 reduction to HOO·. The 2.98 eV stability of Pt–OH relative to HO· lowers the activation energy for reduction of H_2O_2 to HO· + H_2O. The activation barriers for HOO· reduction to H_2O_2 are also lowered even though H_2O_2 bonds to the Pt atom relatively weakly, 0.52 eV. Comparing the OO bond length in HOO· for the hydrogen–bonded precursor states with and without bonding to Pt in Table III, it is seen

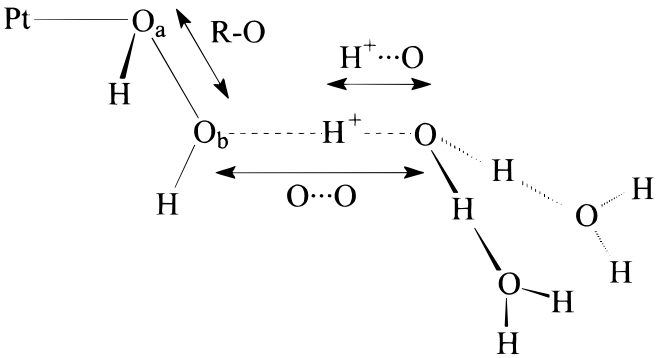

Figure 1. Structure and parameter definitions of reaction complexes illustrated schematically for the case of H_2O_2.

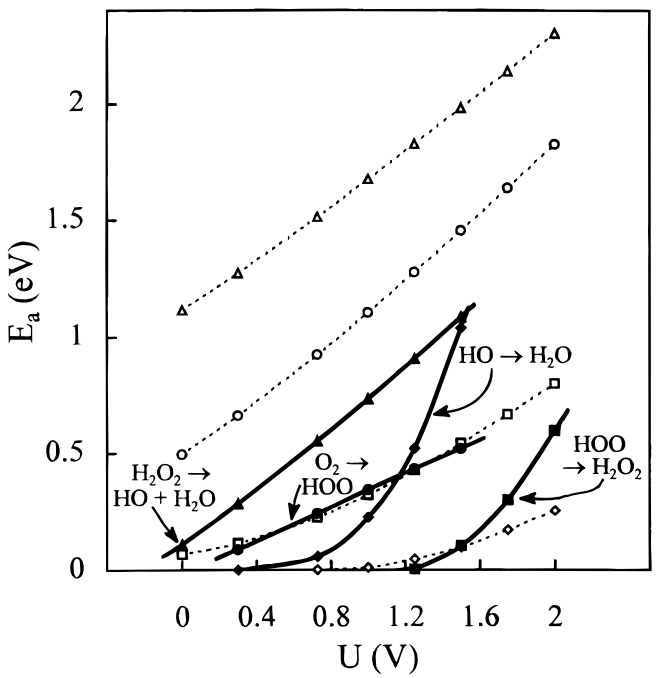

Figure 2. Activation energy, E_a, for the four steps of oxygen reduction to water, Eq. 1–4 as functions of electrode potential, *U*. Heavy lines connect points with species undergoing reduction bonded to a platinum atom, Eq. 9–12. Dotted lines connect points with no bonding to platinum. The same key applies to both sets of curves.

S0013-4651(00)05-094-1 CCC: $7.00

Table II. Pt-OR bond strength (eV) for species discussed in the text. The experimental Pt–O singlet value is 3.82 eV (footnote c of Table I).

	Symmetry	Electronic state[a]	Bond strength
Pt–OO (T-shaped)	C_{2v}	$^1A_1$	0.887
Pt–OO (bent)	C_s	$^1A'$	0.521
Pt–OOH	C_1	^2A	1.827
Pt–OHOH	C_1	^1A	0.521
Pt–O	Linear	$^3\Sigma_g^-$[b]	3.678
Pt–O	Linear	Singlet[c]	3.262
Pt–OH	C_s	$^2A''$	2.984
Pt–OH_2	C_s	$^1A'$	0.567

[a] The singlet state molecules are calculated with the spin-restricted formalism.
[b] The valence orbital α spin occupation is $\sigma\pi\pi\sigma\pi\pi\delta\delta\sigma$, and the β spin occupation is $\sigma\sigma\pi\pi\delta\delta\sigma$.
[c] The symmetry of this state is unidentified in *Gaussian 94* and *Gaussian 98* output.

that bonding to Pt causes the O–O bond to stretch to 1.504 Å, 0.192 Å more than the outer–sphere value. This is 0.04 Å longer than the O–O bond length in H_2O_2, indicating that PtOOH is activated for reduction. The hydrogen–bonded Pt–OHOH precursor also has a long O–O bond, 0.51 Å greater than for the outer-sphere structure, indicating a structural role in its activation too. Finally, Pt–OH is harder to reduce because of the high strength of this Pt–O bond. Table III also shows that the $RO\cdots H^+$ precursor hydrogen bonds are much stronger and shorter when the oxygen is bonded to Pt.

Electrode–potential–dependent trends in structure variables at the transition state may be seen in the data in Table IV. As the potential is increased, it is generally necessary to stretch the $H^+\cdot\cdot\cdot OH_2$ bond more and the $RO\cdots H^+$ distance becomes shorter. The O–O distances generally lengthen. These changes cause the electron affinity of the reaction complex to increase to the prescribed value.

In the transition state structures, before electron transfer and reduction, the calculated Pt Mulliken charge is positive in the range 0.95 to 1.04 for PtO_2, 0.60 to 0.67 for PtOOH, 0.73 to 0.91 for PtH_2O_2, and 0.66 to 0.78 for PtOH for $U = 0.727$ to 1.5 V. After electron transfer the ranges are 0.14 to 0.28 for PtO_2, −0.28 to −0.23 for PtOOH, −0.10 to −0.06 for PtH_2O_2, and 0.29 to −0.18 for PtOH. From this it is seen that, when electron transfers, most of the charge goes to the Pt atom and the remaining amount goes to the oxygen species and associated hydronium ion. This additional electron is mainly in a Pt s-type orbital and, as the reaction proceeds, it moves from Pt to the molecule that is bonded to it. Since the O–O bond is stretched more in transition states with Pt present compared to when it is not, it may be wondered what is the effect of this bond stretch on the electron affinity if the Pt is absent. Is it higher? For O_2 reduction at 0.727 V it is. The $O–O\cdots H^+\cdots OH_2(OH_2)_2$ fragment alone has an electron affinity of 6.634 eV compared to 5.372 eV when bonded to Pt. This structure is, however, 2.063 eV less stable than the outer–sphere precursor structure, and therefore it is not accessible for the outer–sphere reaction. Bonding to Pt reduces the electron affinity of this fragment because Pt donates charge to the oxygen atoms. The Pt–O_2 fragment, in the $U = 0.727$ V transition state structure, has an electron affinity of 0.864 eV, and $H^+\cdots OH_2(OH_2)_2$ in this structure has an electron affinity of 1.522 eV, which shows how the field of the hydronium ion increases the electron affinity of PtO_2, a trend also noted in the outer-Helmholtz–plane study.[13]

An alternative path considered was the one for which Pt–OOH is to be reduced to Pt–O

$$Pt–OOH + H^+(aq) + e^-(U) \rightarrow Pt–O + H_2O(aq) \qquad [13]$$

Calculated activation energies for this, given in Table IV, are much higher than those calculated for the H_2O_2 formation, making this pathway uncompetitive. However, as Table IV shows, should Pt–O form, its reduction to Pt–OH

$$Pt–O + H^+(aq) + e^-(U) \rightarrow Pt–OH \qquad [14]$$

is assured due to very low activation barriers.

The relative overall energetics for two reduction sequences, Eq. 9–12, and Eq. 9, 13, 14, and 12, which include hydrogen–bonded reduction precursor and transition states are presented in Fig. 3 and 4, respectively. Because of cancellation of errors in the solvation model that was discussed in Ref. 13, the overall reaction energy is zero at about $U = 1.12$ V, incorrectly reported as 1.18 in Ref. 13, which is quite close to the 1.23 V reversible potential. As may be seen in Fig. 3, reducing PtOH to $PtOH_2$ is overall uphill in energy by 1–2 eV. The transition state energies shown in Fig. 3 and 4 correspond to energies and structures at which electron transfer occurs and, following this, it costs energy to remove the rigid $OH_2(OH_2)_2$ fragment. Full optimiza-

Table III. Calculated key internuclear distances, *R* (Å), and hydrogen bond strengths, E_{hb} (eV), for Pt-bonded hydrogen-bonded reduction precursors. Outer–sphere results are in parentheses.

System	R(H^+–O)	R(O· · ·H^+)	R(O–O)	R(Pt–O) or R(O–H)	E_{hb}
Pt–O–O· · ·H^+–$OH_2(OH_2)_2$	1.00 (0.97)	1.63 (2.20)	1.3063 (1.2172)	—	0.115 (0.047)
H–O–O· · ·H^+–$OH_2(OH_2)_2$ Pt	1.02 (0.98)	1.52 (1.83)	1.5040 (1.3124)	—	1.090 (0.444)
H H–O–O· · ·H^+–$OH_2(OH_2)_2$ Pt	1.02 (0.98)	1.55 (1.76)	1.9720 (1.4606)	—	1.417 (0.417)
H–O· · ·H^+–$OH_2(OH_2)_2$ Pt	1.05 (0.99)	1.45 (1.76)		1.9875 (0.9771)	0.935 (0.565)
H Pt–O–O· · ·H^+–$OH_2(OH_2)_2$	1.00	1.68	1.5060	—	0.136
Pt–O· · ·H^+–$OH_2(OH_2)_2$	1.02	1.54	—	1.8298	0.635

S0013-4651(00)05-094-1 CCC: $7.00

tion and solvation of the $OH_2(OH_2)_2$ part would be expected to lower the energy requirement for this last step. For the surface oxide pathway, Fig. 4, the activation energies for the first two reduction steps, Eq. 9 and 13, essentially add to give a high overall activation energy for this pathway. The PtO that forms is very reactive, with zero or very small activation energy for reduction to PtOH.

At 1.23 V the experimental activation energy is 0.44 eV over the three low–index platinum surfaces in 0.05 M H_2SO_4(aq).[1,6] An activation energy value of 0.45 eV has been determined for O_2 reduction in a pH 1.9 perchloric acid solution over polycrystalline platinum electrodes.[32] Over the past 30 years a range of activation energies, from 0.11 to 0.99 eV for O_2 reduction over various platinum–containing catalysts in various acid and acid–polymer electrolytes has been reported for the reversible and other potentials.[6,32-47] The values are given in Table V along with electrode, electrolyte, and temperature information. In all of these studies it is asserted that the first one-electron transfer step is rate–limiting, but it has not always been established whether the reduction is four–electron to water or two–

Table IV. Calculated key transition state internuclear distances, *R* (Å), and activation energies, E_a (eV), at various potentials, *U* (V), for the four steps in O_2 reduction, with reactants bonded to a Pt atom, Eq. 13–18. Transition state structures and energies without the Pt atom are in parentheses.

Reaction	Voltage (V)	$H_2O\cdots H^+$ distance	$H^+\cdots O_2$ distance	$H_3O^+\cdots O_2$ distance	O–O distance	Pt–O distance	O–H distance	Reduction E_a (eV)	Oxidation E_a (eV)
PtOO ↔ PtOOH	0.300	1.06	1.42	2.48	1.3279	1.8482	—	0.089	1.254
		(1.06)	(1.42)	(2.48)	(1.2482)			(0.662)	(0.771)
	0.727	1.12	1.31	2.43	1.3474	1.8482	—	0.242	0.982
		(1.09)	(1.35)	(2.44)	(1.2576)			(0.924)	(0.606)
	1.000	1.16	1.25	2.41	1.3554	1.8482	—	0.344	0.810
		(1.11)	(1.31)	(2.42)	(1.2641)			(1.105)	(0.514)
(O_2 ↔ OOH)	1.250	1.20	1.21	2.41	1.3640	1.8482	—	0.433	0.649
		(1.14)	(1.27)	(2.41)	(1.2656)			(1.277)	(0.436)
	1.500	1.24	1.17	2.41	1.3715	1.8482	—	0.520	0.485
		(1.17)	(1.24)	(2.41)	(1.2698)			(1.455)	(0.364)
PtOOH ↔ PtOHOH	0.727	0.97	2.16	3.13	1.5045	2.0149	—	0.000 [a]	0.972
		(1.02)	(1.52)	(2.54)	(1.3613)			(0.226)	(1.539)
	1.000	0.99	0.78	2.77	1.5130	2.0149	—	0.000 [a]	0.495
		(1.04)	(1.46)	(2.50)	(1.3676)			(0.322)	(1.363)
	1.250	1.03	1.50	2.53	1.5128	2.0149	—	0.003	0.174
		(1.06)	(1.41)	(2.47)	(1.3725)			(0.426)	(1.217)
(OOH ↔ HOOH)	1.500	1.12	1.28	2.40	1.5035	2.0149	—	0.104	0.023
		(1.08)	(1.37)	(2.45)	(1.3801)			(0.542)	(1.082)
	2.000	1.24	1.16	2.40	1.5392	2.0149	—	0.597	0.000 [a]
		(1.12)	(1.30)	(2.42)	(1.3975)			(0.799)	(0.840)
PtOHOH ↔	0.000	1.10	1.32	2.42	1.9402	1.8645	—	0.109	2.453
		(1.08)	(1.35)	(2.43)	(1.7572)			(1.116)	(1.869)
PtOH + OH_2	0.300	1.19	1.22	2.41	1.9356	1.8645	—	0.284	2.328
		(1.10)	(1.32)	(2.42)	(1.7771)			(1.274)	(1.727)
	0.727	1.29	1.13	2.42	1.9452	1.8645	—	0.551	2.168
		(1.13)	(1.27)	(2.40)	(1.8018)			(1.514)	(1.540)
	1.000	1.35	1.09	2.44	1.9546	1.8645	—	0.733	2.077
		(1.15)	(1.25)	(2.40)	(1.8209)			(1.675)	(1.428)
(H_2O_2 ↔ OH + OH_2)	1.250	1.39	1.07	2.46	1.9718	1.8645	—	0.906	2.000
		(1.16)	(1.23)	(2.39)	(1.8425)			(1.826)	(1.329)
	1.500	1.42	1.06	2.48	1.9922	1.8645	—	1.085	1.929
		(1.18)	(1.21)	(2.39)	(1.8585)			(1.981)	(1.234)
PtOOH ↔	0.000	1.10	1.35	2.45	1.5339	1.6758	—	0.244	3.328
PtO + OH2	0.300	1.18	1.23	2.41	1.5569	1.6758	—	0.510	3.295
	0.727	1.31	1.12	2.43	1.5920	1.6758	—	0.816	3.174
	1.000	1.34	1.10	2.44	1.6194	1.6758	—	0.973	3.057
	1.250	1.35	1.09	2.44	1.6467	1.6758	—	1.089	2.925
	1.500	1.32	1.11	2.43	1.6777	1.6758	—	1.182	2.766
PtO ↔ PtOH	0.727	1.01	1.60	2.61	—	1.8783	—	0.000 [a]	1.499
	1.000	1.01	1.58	2.59	—	1.8527	—	0.000 [a]	1.211
	1.250	1.02	1.57	2.57	—	1.8380	—	0.000 [a]	0.955
	1.500	1.02	1.56	2.56	—	1.8228	—	0.001	0.705
	2.000	1.05	1.50	2.50	—	1.7851	—	0.031	0.236
PtOH ↔ $PtOH_2$	0.300	0.99	1.72	2.71	—	1.9732		0.000 [a]	0.566
		(0.97)	(1.98)	(2.95)			(0.9878)	(0.000) [a]	(2.740)
	0.727	1.14	1.27	2.41	—	2.0113		0.058	0.115
		(0.99)	(1.78)	(2.77)			(0.9686)	(0.002)	(2.278)
	1.000	1.32	1.11	2.43	—	2.0128		0.225	0.008
		(1.00)	(1.66)	(2.66)			(0.9818)	(0.011)	(2.014)
(OH ↔ OH_2)	1.250	1.58	1.02	2.60	—	2.0038		0.521	0.000 [a]
		(1.02)	(1.58)	(2.60)			(0.9666)	(0.047)	(1.799)
	1.500	1.95	0.98	2.93	—	1.9844		1.039	0.000 [a]
		(1.03)	(1.49)	(2.52)			(0.9788)	(0.098)	(1.601)

[a] Electron transfers before H-bonded complex (precursor complex) is formed.

S0013-4651(00)05-094-1 CCC: $7.00

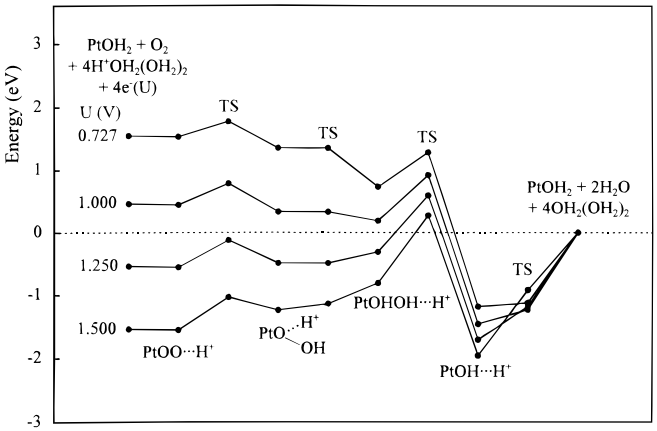

Figure 3. Energies as functions of electrode potential for O_2 reduction reaction system passing through the peroxide pathway, Eq. 9–12. TS and hydrogen–bonded reduction precursor, R–O· · ·H^+–OH_2, energies are connected.

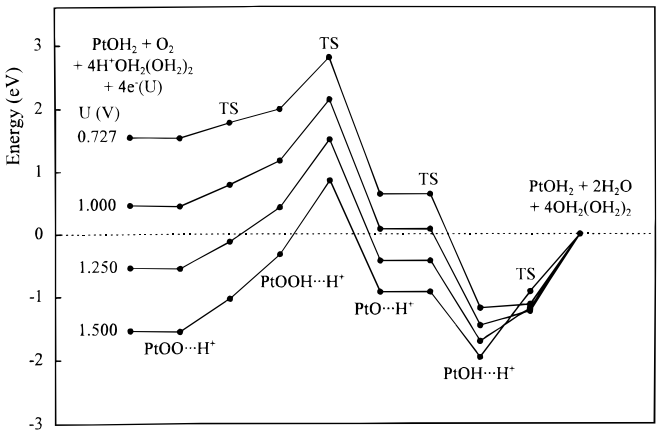

Figure 4. For O_2 reduction as in Fig. 3 except passing through Eq. 9, 13, 14, 12, the oxide pathway.

electron to hydrogen peroxide. The experimental results for clean platinum in weak acid, 0.44 eV [6] and 0.45 eV, [32] seem to be most appropriate for comparison to the results calculated here. The calculations yield 0.43 eV for Pt–OOH formation beginning with end–on bonded O_2. If the O_2 is initially in the more stable side–on configuration, the activation energy is about 0.80 eV, assuming the same hydrogen–bonding stabilization in the precursor for side–on O_2 as calculated for the end–on structure. Both are close to the experimental value for the four–electron process, but an accurate determination of the activation energy for side–on O_2 will require larger models.

Table V. Experimentally determined apparent enthalpy of activation, ΔH^*, at various platinum/acid-electrolyte interfaces

ΔH* (eV)	Electrode	Electrolyte	Temp. range (°C)	Ref.
0.57[a]	Oxide-covered Pt foil	85% H_3PO_4	25-136	33
0.99[a]	Oxide-free Pt foil	85% H_3PO_4	25-136	34
0.64[a]	Active Pt foil	85% H_3PO_4	25-136	35
0.55[a]	Pt foil	1.1 M F_3C-SO_3H	0-62	36
0.43[a]	Prereduced Pt disk	85% H_3PO_4	25-150	37
0.34[a]	Reduced Pt disk	85% H_3PO_4	25-70	38
0.87[a]	Oxide-covered Pt	9.5 M F_3C-SO_3H	25-80	39
0.24[a]	Oxide-free Pt	9.5 M F_3C-SO_3H	25-80	39
0.62[a]	Oxide-covered Pt	$HClO_4$ sol (pH=1.9)	5-45	32
0.45[a]	Oxide-free Pt	$HClO_4$ sol (pH=1.9)	5-45	32
0.75[a]	Pt microelectrode	98% H_3PO_4	25-150	40
0.18[a]	Pt microelectrode	9.5 M F_3C-SO_3H	35-90	41
0.21[a]	Pt microelectrode	6.0 M F_3C-SO_3H	25-73	41
0.30[a]	Pt microelectrode	3.0 M F_3C-SO_3H	25-69	41
0.26[b]	Oxide-free Pt	$HClO_4$ sol (pH=1.9)	5-45	42
0.76[a]	Oxide-covered Pt microelectrode	Nafion® 117	30-80	43
0.29[a]	Oxide-free Pt microelectrode	Nafion® 117	30-80	43
0.87[a]	Pt/C-Nafion unimpregnated	Nafion® 117	25-80	44
0.95[a]	Pt/C-Nafion impregnated	Nafion® 117	25-80	44
0.81[a]	Pt-Nafion impregnated	Nafion® 117	25-80	44
0.76[a]	Pt microelectrode	Nafion® 117	25-80	44
0.51[a]	Pt(111) disk	1.0 M H_2SO_4	8-62	45
0.11[a]	Pt(100) disk	1.0 M H_2SO_4	8-62	45
0.64[c]	Pt/Carbon	Nafion® 117	35-80	46
0.30[c]	Pt-Cr/Carbon	Nafion® 117	35-80	46
0.29[c]	Pt-Cr/Carbon	Nafion® 117	35-80	46
0.25[c]	Pt-Co/Carbon	Nafion® 117	35-80	46
0.37[c]	Pt-Co/Carbon	Nafion® 117	35-80	46
0.25[c]	Pt-Ni/Carbon	Nafion® 117	35-80	46
0.45[c]	Pt-Ni/Carbon	Nafion® 117	35-80	46
0.44[a]	Pt(111) disk	0.05 M H_2SO_4	25-60	6
0.44[a]	Pt(110) disk	0.05 M H_2SO_4	25-60	6
0.44[a]	Pt(100) disk	0.05 M H_2SO_4	25-60	6
0.57[a]	Oxide-covered Pt microdisk	Nafion® 117	30-70	47
0.60[a]	Oxide-free Pt microdisk	Nafion® 117	30-70	47
0.25[a]	Oxide-covered Pt microdisk	BAM® 407	30-70	47
0.41[a]	Oxide-free Pt microdisk	BAM® 407	30-70	47

[a] Determined from the slope of log i_0 *vs.* 1/*T*.
[b] Determined at 0.8 V.
[c] Determined from the slope of log *i*(at 0.9 V) *vs.* 1/*T*.

S0013-4651(00)05-094-1 CCC: $7.00

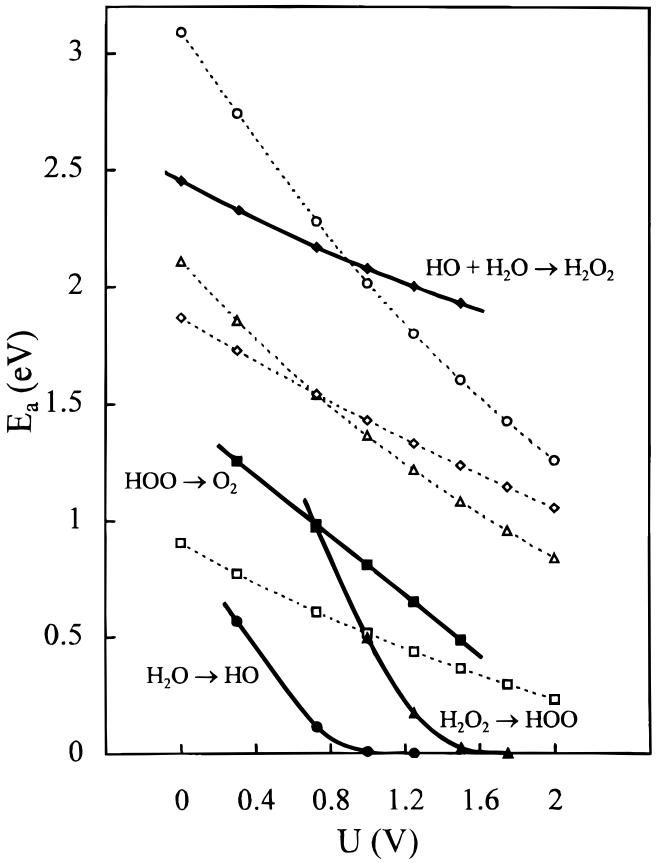

Figure 5. As in Fig. 2 but for steps in water oxidation to O_2.

The calculated activation energy for Pt–OHOH reduction at 1.23 V is rather high at 0.91 eV, and the Pt–O bond strength is weak at 0.52 eV, suggesting that surface sites that are only able to adsorb O_2 end–on are responsible for H_2O_2 production. The active site for the four-electron process probably requires an ensemble of two or more unblocked adjacent platinum atom sites, and in this case OO bond cleavage may accompany or follow the first reduction step. The present calculations indicate that if this occurs, the resulting O(ads) and OH(ads) will undergo reduction to water with very low activation energies. A theoretical study of the four-electron process with a model providing two adjacent adsorption sites on platinum is underway.[48]

Water oxidation.—Potential–dependent activation energies for water oxidation to oxygen, the reverse of Reactions 9–12, are shown in Fig. 5. In this case, the oxidation precursor structures have the $OH_2(OH_2)_2$ fragment, fixed in the previously determined structure, hydrogen bonded to the reactants. Structure and hydrogen–bond strengths for these precursors are in Table VI. Bonding to platinum greatly decreases the activation energies for H_2O and H_2O_2 oxidation steps but increases them for HO· and HOO· oxidation steps. The high stabilities of the Pt–OH and Pt–OOH bonds correlate with these findings.

Figure 6 illustrates the relative energy changes for the four oxidation steps through the peroxide pathway at the four electrode potentials modeled. The hydrogen–bonded precursors for Pt–OH_2 oxidation have potential dependent energies because the oxidative electron transfer has taken place before the hydrogen–bond formation between Pt–OH_2 and $OH_2(OH_2)_2$ is completed for the 1.50 and 1.25 V potentials. The precursors are positively charged in these two cases. Comparing Fig. 6 for the peroxide pathway and Fig. 7 for the oxide pathway it may be seen the Pt–O oxidation to Pt–OOH has extremely high activation barriers, around 3.0 eV, which negates the possibility that Pt–O, if it forms, can be further oxidized by direct bonding to the hydroxide oxygen. However, the activation energies for forming Pt–O from Pt–OH are smaller than those for forming Pt–OHOH in the potential region of water oxidation, and this implies that other pathways involving surface recombination of adsorbed oxygen species may be considered. Definitive modeling of such recombinations demands the use of extended surface models. Nevertheless, interesting speculations based on bond strengths are possible. The Pt–OH bond strength is 2.5 eV on platinum surfaces at low coverage but drops to 1.5 eV at high coverage.[26] Electrochemical measurements have yielded ~1.4 eV for the Pt–OH bond strength at 0.5 monolayer coverage.[49] The Pt–O bond strength has been determined to be ~3.5 eV at 0.5 monolayer coverage. Based on these numbers and a calculated O–O bond strength in HOO· of 2.62 eV, and the calculated Pt–OOH bond strength, it is estimated that adsorbed O and OH probably do not combine to form adsorbed

Table VI. Calculated key internuclear distances, *R* (Å), and hydrogen bond strengths, E_{hb} (eV), for Pt-bonded hydrogen-bonded oxidation precursors formed by the $OH_2(OH_2)_2$ water trimer approaching the PtO_xH_y species. Outer–sphere results are in parentheses.

System	R(H· · ·O)	R(O–H)	R(O–O)	R(Pt–O) or R(O–H)	E_{hb}
Pt–O–O–H···$OH_2(OH_2)_2$	1.55 (1.50)	1.02 (1.03)	1.4477 (1.3190)	—	0.842 (1.077)
H–O–O–H···$OH_2(OH_2)_2$ | Pt	1.22 (1.62)	1.17 (1.00)	1.4999 (1.4700)	—	0.597 (0.794)
H | H–O–O–H···$OH_2(OH_2)_2$ | Pt	1.75 (1.73)	0.98 (0.99)	10.0[a] (2.7779)	—	0.628 (0.671)
H–O–H···$OH_2(OH_2)_2$ | Pt	1.39 (1.73)	1.07 (0.98)	—	2.0184 (0.9599)	1.243 (0.678)
H | Pt–O–O–H···$OH_2(OH_2)_2$	1.74	0.98	10.0[a]	—	0.608
Pt–O–H···$OH_2(OH_2)_2$	1.58	1.02	—	1.9172	0.605

[a] Value 10.0 for separated, noninteracting compounds.

S0013-4651(00)05-094-1 CCC: $7.00

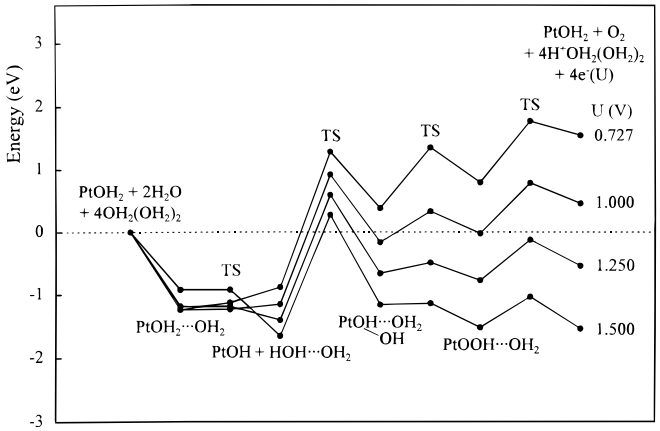

Figure 6. As in Fig. 3 but for water oxidation to O_2 via the peroxide pathway. TS and hydrogen–bonded oxidation precursor, R–O–H· · ·OH_2, energies are connected.

HOO·. Conversely, once adsorbed HOO· forms during reduction, it is likely to be quickly reduced to $2H_2O$ if the surface conditions allow it to dissociate. Adsorbed OH at high coverage might be able to combine to form bridging H_2O_2 if its adsorption bond strength is around 1.0 eV. However, even at high coverage these energies do not favor combination of adsorbed O to form gas phase O_2.

Reversible potentials for the formation of intermediates in aqueous solution and when bonded to Pt—As was noted in Ref. 13, for five reduction reactions involving H_xO_y species for which the reversible potentials are known, the reversible potentials calculated based on the reaction energy differences are, on average, 0.49 V below the measured values. This means that there is a near constancy in the $T\Delta S$, solvation, and zero–point energy contributions that must be added to reaction energies to yield reaction Gibbs energies for use in evaluating reversible potentials. Empirically based estimates of these contributions resulted in predictions on average 0.05 V below the measured values. Table VII gives predicted reversible potentials for reduction Reactions 1–4, which are outer-Helmholtz plane, and Reactions 9–14, with the reactants and products bonded to a Pt atom. These predictions are from the calculated reaction energies with a 0.49 V correction. Comparison of the predictions with the experimental results for which standard states and Gibbs energy changes are verifiable, the exceptions being HOO· and Pt–bonded species, shows the possibility of making reversible potential predictions with an accuracy of 0.2 V.

A number of comments can be made about the results in Table VII. Bonding to Pt increases the reversible potential for the first reduction of O_2 because of the relatively greater strength of the Pt–OOH bond compared to the Pt–OO bond. By the same token, the next reduction has a decreased reversible potential because H_2O_2 bonds weakly to Pt. The third reduction has a high reversible potential because of the high strength of the Pt–OH bond, and this strength is also responsible for the large decrease in the reversible potential for the last step. It is of particular note that the reversible potential predicted for OH(ads) formation from H_2O(ads) is 0.57 V, close to the ~0.5–0.6 V potential at which OH(ads) begins to form on the low-index platinum surfaces in 0.1 M perchloric acid.[2] The 3.06 V reversible potential for PtOHOH reduction to PtOH indicates that reduction of H_2O_2 is strongly favored thermodynamically if it has a Pt site to adsorb on. The 1.32 V PtO to PtOH reduction potential says that oxidation of PtOH will take place at a potential about 0.75 V more positive than its formation potential in acid solution.

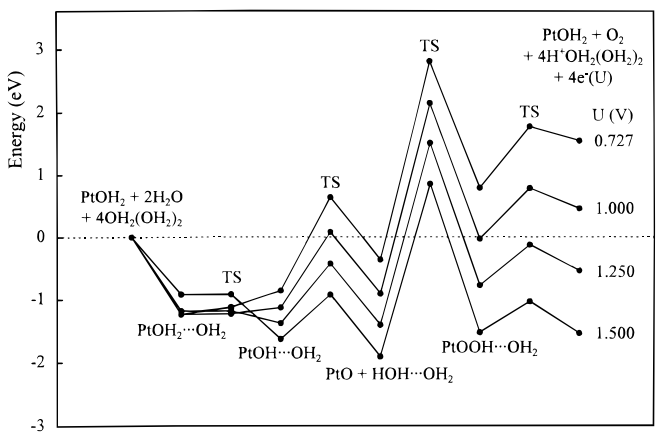

Figure 7. As in Fig. 4 but for water oxidation to O_2 via the oxide pathway.

Tafel slopes.—The assumption of a linear dependence of the Gibbs activation energy on the applied electrode potential at constant temperature yields the Butler-Volmer equation relating the current density to the overpotential.[14] This model also assumes that an overpotential decreases the activation Gibbs energy for the reaction in one direction and increases it for the reverse direction. The Butler-Volmer equation provides a model for determining the potential dependence of the activation enthalpy and also the activation energy, for reasons discussed above, provided the activation entropy is not dependent on temperature and potential. In this case, the increase in the activation enthalpy from its value at the reversible potential is $\beta F\eta$ for the reduction reaction, where β is a constant, F is Faraday's constant, and η is the overpotential for oxidation. Then the decrease in activation enthalpy for the oxidation reaction is $-\alpha F\eta$ where $\alpha = 1 - \beta$. The Butler–Volmer equation is then

$$j = j_o[e^{\alpha F\eta/RT} - e^{-\beta F\eta/RT}] \quad [15]$$

where j_o is the exchange current density. Thus, when the above conditions hold, the calculated potential–dependent activation energies can be used to predict β and α and may provide insight into Tafel plots.

As may be seen on comparing Fig. 2 and 5, for PtOH reduction the slope of activation energy *vs*. potential, β, exceeds unity at potentials exceeding ~1 V and the same is true for PtOOH reduction at high potentials. The slopes of the corresponding oxidation activation energies, α, decrease to zero in the ranges where β exceeds 1; in fact, the activation energies drop to zero in these ranges. These results are caused by the loss of a strong Pt–O bond in these two reduction steps or, conversely, by the gain of a strong PtO bond in the two oxidation steps. Potential-dependent structure-bond energy relationships are responsible for this non-Butler-Volmer behavior. In these cases α +

Table VII. Reversible potentials, U^o(V) as calculated from total energies as discussed in the text. Experimental values are in parentheses.

Reaction	U^o	U^o(expt)[a]
$O_2 + H^+(aq) + e^-(U^o) \rightleftharpoons HOO$	−0.52	(−0.125)[b]
$HOO + H^+(aq) + e^-(U^o) \rightleftharpoons H_2O_2$	1.79	(1.515)[b]
$H_2O_2 + H^+(aq) + e^-(U^o) \rightleftharpoons HO + H_2O$	0.60	(0.713)[c]
$HO + H^+(aq) + e^-(U^o) \rightleftharpoons H_2O$	2.99	(2.813)[c]
$PtOO + H^+(aq) + e^-(U^o) \rightleftharpoons PtOOH$	0.42	
$PtOOH + H^+(aq) + e^-(U^o) \rightleftharpoons PtOHOH$	0.48	
$PtOHOH + H^+(aq) + e^-(U^o) \rightleftharpoons PtOH + H_2O$	3.06	
$PtOH + H^+(aq) + e^-(U^o) \rightleftharpoons PtOH_2$	0.57	
$PtOOH + H^+(aq) + e^-(U^o) \rightleftharpoons PtO + H_2O$	2.22	
$PtO + H^+(aq) + e^-(U^o) \rightleftharpoons PtOH$	1.32	

[a] J. P. Hoare, in *Standard Potentials in Aqueous Solution*, A. J. Bard and J. Jordan, Editors, Marcel Dekker, New York (1985), Ref. 29.
[b] This value is not verifiable from tables of reaction free energies in footnote a.
[c] This value is verifiable from tables of reaction free energies in footnote a.

S0013-4651(00)05-094-1 CCC: $7.00

$\beta \neq 1$ because the activation energy increases faster than the increase in potential in these ranges.

The β predicted for PtOO reduction to PtOOH is about 0.37 in the O_2 reduction overpotential region, less than the value of 0.5 measured and ascribed to this reaction,[1,6] but, as discussed in the Results and Discussion section, the mechanism probably requires a dual Pt adsorption site, which is currently under investigation.[48] For PtOHOH reduction to PtOH + H_2O the β is predicted to be larger, 0.67 in this potential range. It is notable that the activation energy for PtOH reduction to $PtOH_2$ increases rapidly with potential and if it surpasses the activation energy for the first step in PtO_2 reduction, it may be evaluated as a candidate for the cause of the change in Tafel slope at ~0.8 V that has been observed during four-electron reduction of O_2.[1,6]

Electron potential between the electrode surface and the outer–Helmholtz plane.—To establish thermodynamic equilibrium at an electrode-electrolyte interface, the electrode surface may take on a net positive or negative charge which is compensated by ions in the double-layer region so there is no net charge on the interfacial system. Beyond the diffuse region, the electrolyte bears no net charge and the reacting ions migrate through a charge compensating background of counterions. The charge concentration on the electrode surface can be quantified by capacitance measurements, but the distribution of compensating charge is difficult to measure. If the electrode potential is set at the potential of zero charge (pzc), the electrode surface is essentially uncharged and, due to the absence of an electric field, an electron or ion can pass through the interface without the involvement of electrostatic work on it or by it. At potentials away from the pzc a potential–dependent electrostatic field will extend from the electrode surface to the outer–Helmholtz–plane and will extinguish in the diffuse region of compensating charge just beyond. The charged components of a redox couple will, when added to the solution with a double–layer field present, assume concentration gradients and participate in the charge distribution in the double–layer region, possibly perturbing the double–layer field and pzc. Assuming that a rigid double–layer field exists, an ion passing through some or all of the double layer to react will generate or consume electrostatic work.

Little is known quantitatively about the double–layer electric field model, and it must be emphasized that, since the double layer is the order of a few atomic diameters thick, the assumption of a homogenous electric field is so crude that the model may not be a suitable zeroth order starting point. Measurements, as reviewed recently by Fawcett,[50] give evidence for the double–layer potential drop having substantial kinetic effects on reactions in the double–layer region. However, Koper and Schmickler in their recent theoretical work on inner-Helmholtz–plane redox reactions[51] have not incorporated the potential drop across the double layer, arguing that, at several tenths of an electron volt, it is small. In the context of understanding electrocatalysis such a drop is probably not insignificant. Even at the outer–Helmholtz–plane there is a potential drop. Using a classical model, Calvo[52] found a variation of $\pm \leq 0.2$ V in the potential at the outer-Helmholtz–plane relative to the bulk solution for a 1 V range above and below the pzc for low 1.0 mM aqueous ion concentration. At high 1.0 M concentration the variation was $\pm \leq 0.1$ V, in fact small. Halley, Price, and co-workers[53] have recently predicted, using molecular dynamics and quantum calculations, considerable structure in the time-averaged electrostatic potentials in the double–layer region over a copper plate in water where the compensating charge was on another copper plate several molecular diameters away. When smoothed, the field decreased upon approaching either surface and the potential drop from each surface to several angstroms into the water was small. In the bulk water region the potential changed nearly linearly between the plates. Whether high ionic concentrations would result in a higher double–layer potential drop could not be determined due to computer limitations.

One can anticipate the effect of a double–layer potential drop for a nonequilibrium situation where net current flows. Consider positive species undergoing reduction, such as $[OO\cdot\cdot\cdot H\cdot\cdot\cdot OH_2(OH_2)_2]^+$, which is abbreviated as $O_2 + H^+$ in the following discussion, with the electrode potential negative of the pzc, so that the electrode surface is then negatively charged. Let the electrode be in the overpotential region for oxygen reduction. Suppose an $O_2 + H^+$ species in the double layer is thermally agitated and becomes reduced. To sustain a current flow, another $O_2 + H^+$ species will diffuse from nearby in the outer–Helmholtz–plane to replace it and the vacancy thus formed in the outer–Helmholtz–plane will be replaced by an $O_2 + H^+$ from the diffuse layer which will be replaced by $O_2 + H^+$ from the bulk electrolyte and the proton vacancy will diffuse to the anode where it will be replaced by a newly generated proton. Let E_a be the electron affinity of $O_2 + H^+$ in a given structure when in the bulk solution. Denoting this $O_2 + H^+$ as R^+

$$R^+ + e^+ \rightarrow R + E_a \qquad [16]$$

where E_a is the heat liberated. When R^+ is in the double layer

$$R^+_{dl} + e^- \rightarrow R_{dl} + E'_a \qquad [17]$$

where E'_a is its electron affinity in this position. Since the electrode surface is negatively charged, it is reasonable to assume that R^+ is attracted to the double–layer position and, losing potential energy, it should release heat q

$$R^+ \rightarrow R^+_{dl} + q \qquad [18]$$

Combining Eq. 16–18 yields

$$E'_a = E_a - q \qquad [19]$$

which means that the electron affinity of the $O_2 + H^+$ reduction center in the double–layer region is reduced by the heat evolved when $O_2 + H^+$ diffuses from the bulk solution to this position. This heat will not ordinarily couple with the activation step, and so it will contribute to the resistance of the half cell. For $O_2 + H^+$ in the double layer there are two ways to initiate the reduction: (*i*) by thermal agitation to a structure with increased electron affinity but unfortunately higher energy and (*ii*) by decreasing the electrode potential to increase its reducing capability. Thus, in this case, the double layer makes two contributions to the need to run the half-cell at higher overpotentials to maintain desired current flow.

When the electrode potential is positive of the pzc, there is a heat of activation for R^+ entering the double-layer region, and q changes sign so the complex to be reduced will have a larger electron affinity in the double–layer region, which will result in a lower activation energy for reduction compared to that in the bulk solution. For a given overpotential, the first effect will decrease the current and the second one will increase it.

From what is said above, it may be speculated that for reactions in the double layer, with all else being equal, reduction currents at low overpotential, for which the double layer is little perturbed, may be higher for electrodes with pzc negative of the reversible potential, while, for oxidation reactions, electrodes with pzc positive of the reversible potential may present higher currents. An experimental check of this proposition would require a systematic study of reactions over different electrodes of known pzc values. Though much remains to be learned about details of double layers, it is possible to determine the consequence to a calculated activation energy of an assumed double–layer potential drop by simply shifting the potential scale by the assumed potential drop and reading the activation energies of Fig. 2 and 5.

Polarization of adsorbate bonds due to electrode charging.—The effects of electrode–potential-dependent bond polarizations have been studied for almost two decades by means of parametric Fermi level shifts in cluster and slab-band representations of surfaces treated with semiempirical molecular orbital theory.[8,54-56] This is a limited approach useful mainly for predicting and understanding electrode potential dependent trends in the absence of electron transfer;

S0013-4651(00)05-094-1 CCC: $7.00

it is too inaccurate for studying redox reactions in either the inner- or outer-Helmholtz–plane regions.

Bond polarizations are not an issue for outer-Helmholtz–plane charge–transfer reactions and the model for reversible potentials described above works well, limited by the treatment of the solvation of the reactants and the quality of the self-consistent quantum calculations. However, for reactants adsorbed on the electrode surface the bond polarizations will vary with electrode potential. A complete *ab initio* model for this would have to include surface charges and double–layer ions and molecules. Studying electrode potential dependencies of electrocatalytic reactions this way is not currently a tractable approach, though advanced computers used with *ab initio* quantum mechanics and molecular dynamics software may allow such modeling in the future. The authors believe, however, that it is worthwhile to make studies of the electrode potential dependence of electrocatalytic mechanisms and activation energies to determine structure and electronic factors in the absence of bond polarizations as is developed here. The electron transfer will take place when the reaction center, including the surface, is thermally excited to an activated structure with an electron affinity corresponding to the desired electrode potential, including possible double–layer potential drop, just as in the outer–Helmholtz–plane studies. The effects of potential–dependent adsorbate bond polarizations, such as bond weakenings, may be, when known, added as a perturbation to the zeroth order approach.

Acknowledgment

T.V.A. is grateful to the CWRU Department of Chemistry for support. The U.S. A.R.O. partially supported the work through grant no. DAAD 19-99-1-0253. The authors also benefited from a critical reading of the manuscript and calculational assistance by Dr. Reyimjan Sidik.

Case Western Reserve University assisted in meeting the publication costs of this article.

References

1. N. M. Markovic and P. N. Ross, in *Interfacial Electrochemistry: Theory, Experiment, and Applications*, A Wieckowski, Editor, pp. 821-841, Marcel Dekker, New York (1999).
2. R. Adzic, in *Electrocatalysis*, J. Lipkowski and P. N. Ross, Editors, pp. 197-242, Wiley, New York (1998).
3. T. Abe, G. M. Swain, K. Sashikata, and K. Itaya, *J. Electroanal. Chem.*, **382**, 73 (1995).
4. J. X. Wang, N. S. Marinkovic, and R. R. Adzic, *Colloids Surf.*, **134**, 165 (1998).
5. R. R. Adzic and J. X. Wang, *J. Phys. Chem. B*, **102**, 8988 (1998).
6. B. N. Grgur, N. M. Markovic, and P. N. Ross, *Can. J. Chem.*, **75**, 1465 (1997).
7. S. P. Mehandru and A. B. Anderson, *Surf. Sci.*, **216**, 105 (1989).
8. A. B. Anderson, in *Structural Effects in Electrocatalysis and Oxygen Electrochemistry*, D. Scherson, D. Tryk, M. Daroux, and X. Xing, Editors, PV 92-11, pp. 434-439, The Electrochemical Society Proceedings Series, Pennington, NJ (1992).
9. C. F. Zinola, A. J. Arvia, G. L. Estiu, and E. A. Castro, *J. Phys. Chem.*, **98**, 7566 (1994).
10. J. O'M. Bockris and R. Abdu, *J. Electroanal. Chem.*, **448**, 189 (1998).
11. A. B. Anderson and D. B. Kang, *J. Phys. Chem. A*, **102**, 5993 (1998).
12. A. B. Anderson and T. V. Albu, *Electrochem. Commun.*, **1**, 203 (1999).
13. A. B. Anderson and T. V. Albu, *J. Am. Chem. Soc.*, **121**, 11855 (1999).
14. For further discussion, see R. J. D. Miller, G. L. McLendon, A. J. Nozik, W. Schmickler, and F. Willig, *Surface Electron-Transfer Processes*, Section 3.2, VCH, New York (1995).
15. R. A. Marcus and N. Sutin, *Biochim. Biophys. Acta*, **81**, 265 (1985).
16. R. J. D. Miller, G. L. McLendon, A. J. Nozik, W. Schmickler, and F. Willig, *Surface Electron-Transfer Processes*,, Section 3.3, VCH, New York (1995).
17. R. W. Gurney, *Proc. R. Soc. London, Ser. A*, **134**, 137 (1931).
18. N. S. Hush, *J. Electroanal. Chem.*, **470**, 170 (1999).
19. M. T. M. Koper and W. Schmickler, in *Electrocatalysis*, J. Lipkowski and P. N. Ross, Editors, pp. 291-322, Wiley, New York (1998).
20. M. T. M. Koper and G. A. Voth, *J. Chem. Phys.*, **109**, 1991 (1998).
21. M. D. Newton, *Chem. Rev.*, **91**, 767 (1991).
22. J. P. Hoare, *The Electrochemistry of Oxygen*, p. 163, Interscience, New York (1968).
23. J. O'M. Bockris and S. U. M. Khan, *Surface Electrochemistry*, p. 246, Plenum Press, New York (1993).
24. J. O'M. Bockris and S. U. M. Khan, *Surface Electrochemistry*, p. 493, Plenum Press, New York (1993).
25. M. J. Frisch, G. W. Trucks, H. B. Schlegel, P. M. W. Gill, B. G. Johnson, M. A. Robb, J. R. Cheeseman, T. A. Keith, G. A. Petersson, J. A. Montgomery, K. Raghavachari, M. A. Al-Laham, V. G. Zakrzewski, J. V. Ortiz, J. B. Foresman, J. Cioslowski, B. B. Stefanov, A. Nanayakkara, M. Challacombe, C. Y. Peng, P. Y. Ayala, W. Chen, M. W. Wong, J. L. Andres, E. S. Replogle, R. Gomperts, R. L. Martin, D. J. Fox, J. S. Binkley, D. J. Defrees, J. Baker, J. P. Stewart, M. Head-Gordon, C. Gonzalez, J. A. Pople, in *Gaussian 94*, (Revision C. 3) Gaussian, Inc., Pittsburgh, PA (1995).
26. C. E. Mooney, L. C. Anderson, and J. H. Lunsford, *J. Phys. Chem.*, **97**, 2505 (1993).
27. B. A. Sexton and A. E. Hughes, *Surf. Sci.*, **140**, 227 (1984).
28. C. E. Moore, *Atomic Energy Levels*, NBS Circular 467, p. 181, U.S. Government Printing Office, Washington, DC (1958).
29. *Handbook of Chemistry and Physics*, 67th ed., C. R. Weast, Editor, p. E89, CRC Press, Boca Raton, FL (1986).
30. *Handbook of Chemistry and Physics*, 67th ed., C. R. Weast, Editor, p. E63, CRC Press, Boca Raton, FL (1986).
31. A. M. Kuznetsov and W. Lorenz, *Chem. Phys.*, **185**, 333 (1994); A. M. Kuznetsov and W. Lorenz, *Chem. Phys.*, **214**, 243 (1997).
32. D. B. Sepa, M. V. Vojnovic, L. M. Vracar, and A. Damjanovic, *Electrochim. Acta*, **31**, 91 (1986).
33. A. J. Appleby, *J. Electroanal. Chem.*, **24**, 97 (1970).
34. A. J. Appleby, *J. Electrochem. Soc.*, **117**, 328 (1970).
35. A. J. Appleby, *J. Electrochem. Soc.*, **117**, 641 (1970).
36. A. J. Appleby and B. S. Baker, *J. Electrochem. Soc.*, **125**, 404 (1978).
37. J. C. Huang, R. K. Sen, and E. Yeager, *J. Electrochem. Soc.*, **126**, 786 (1979).
38. W. E. O'Grady, E. J. Taylor, S. Srinivasan, *J. Electroanal. Chem.*, **132**, 137 (1982).
39. W. E. O'Grady and J. H. Zagal, *Electrochim. Acta*, **29**, 1609 (1984).
40. B. R. Scharifker, P. Zelenay, and J. O'M. Bockris, *J. Electrochem. Soc.*, **134**, 2714 (1987).
41. M. A. Enayetullah, T. D. DeVilbiss, and J. O'M. Bockris, *J. Electrochem. Soc.*, **136**, 3369 (1989).
42. A. Damjanovic and D. B. Sepa, *Electrochim. Acta*, **35**, 1157 (1990).
43. A. Parthasarathy, S. Srinivasan, A. J. Appleby, and C. R. Martin, *J. Electrochem. Soc.*, **139**, 2530 (1992).
44. A. Parthasarathy, S. Srinivasan, A. J. Appleby, and C. R. Martin *J. Electroanal. Chem.*, **339**, 101 (1992).
45. C. F. Zinola, A. M. Castro Luna, and A. J. Arvia, *Electrochim. Acta*, **39**, 1951 (1994).
46. S. Mukerjee, S. Srinivasan, M. P. Soriaga, and J. McBreen, *J. Phys. Chem.*, **99**, 4577 (1995).
47. P. D. Beattie, V. I. Basura, and S. Holdcroft, *J. Electroanal. Chem.*, **468**, 180 (1999).
48. A. B. Anderson and R. Sidik, Research in progress.
49. N. M. Markovic, T. J. Schmidt, B. N. Grgur, H. A. Gasteiger, R. J. Behm, and P. N. Ross, *J. Phys. Chem. B*, **103**, 8568 (1999).
50. R. W. Fawcett, in *Electrocatalysis*, J. Lipkowski and P. N. Ross, Editors, pp. 323-371, Wiley, New York (1998).
51. M. T. M. Koper and W. Schmickler, in *Electrocatalysis*, J. Lipowski and P. N. Ross, Editors, pp. 291-322, Wiley, New York (1998).
52. E. J. Calvo, *Compre. Chem. Kinet.*, **26**, 1 (1986).
53. S. Walbran, A. Mazzolo, J. W. Halley, D. L. Price, *J. Chem. Phys.*, **109**, 8076 (1998).
54. A. B. Anderson, *J. Catal.*, **67**, 129 (1981).
55. A. B. Anderson, *J. Electroanal. Chem.*, **280**, 37 (1990).
56. A. B. Anderson, in *Interfacial Electrochemistry: Theory, Experiment and Applications*, A. Wieckowski, Editor, pp. 83-96, Marcel Dekker, New York (1999).